

LEGIBILITY NOTICE

A major purpose of the Technical Information Center is to provide the broadest dissemination possible of information contained in DOE's Research and Development Reports to business, industry, the academic community, and federal, state and local governments.

Although a small portion of this report is not reproducible, it is being made available to expedite the availability of information on the research discussed herein.

Received
JUL 10 1989

Los Alamos National Laboratory is operated by the University of California for the United States Department of Energy under contract W-7405-ENG-36

LA-UR--89-1933

DE89 014022

TITLE An Overview of Radiography in Chemical Energy Warhead Research

AUTHOR(S) Dr. Lawrence M. Hull, M-8

SUBMITTED TO 1989 Flash Radiography Topical Symposium, August 15-18, 1989
Wapinitia River Conference Center
Wapinitia, Oregon

DISCLAIMER

This report was prepared as an account of work sponsored by an agency of the United States Government. Neither the United States Government nor any agency thereof, nor any of their employees, makes any warranty, express or implied, or assumes any legal liability or responsibility for the accuracy, completeness, or usefulness of any information, apparatus, product, or process disclosed, or represents that its use would not infringe privately owned rights. Reference herein to any specific commercial product, process, or service by trade name, trademark, manufacturer, or otherwise does not necessarily constitute or imply its endorsement, recommendation, or favoring by the United States Government or any agency thereof. The views and opinions of authors expressed herein do not necessarily state or reflect those of the United States Government or any agency thereof.

By acceptance of this article the publisher recognizes that the U.S. Government retains a nonexclusive, royalty-free license to publish or reproduce the published form of this contribution or to allow others to do so for U.S. Government purposes.

The Los Alamos National Laboratory requests that the publisher identify this article as work performed under the auspices of the U.S. Department of Energy.

MASTER

Los Alamos Los Alamos National Laboratory
Los Alamos, New Mexico 87545



AN OVERVIEW OF RADIOGRAPHY IN CHEMICAL ENERGY WARHEAD RESEARCH

Dr. Lawrence M. Hull
Explosives Applications Group, M-8
Los Alamos National Laboratory, MS J960
Los Alamos, NM 87545
(505) 667-6618

INTRODUCTION

The high-speed objects and the considerable light, dust, and smoke characteristic of a chemical energy warhead test firing necessitate the use of flash radiography as a major diagnostic tool. This paper reviews many of the applications of radiography to chemical warhead studies conducted by many researchers at Los Alamos National Laboratory. Each type of contribution is illustrated by a figure, and the contributors are listed by figure number at the end. The emphasis of the paper is on the relationship between the kind of information obtained and the radiographic technique employed. Details of the techniques are provided only when it is necessary for clarity. A few examples of analysis of the radiographic data are given, but they are in no way exhaustive.

The applications span a wide spectrum of flash x-ray energies and fluence, from 150-keV commercial machines to the 30-MeV, 120-R PHERMEX* machine. Low-energy x rays are useful in the study of small or low-density objects such as highly disrupted penetrators, fragments, or spall. Medium-energy x rays are useful when blast and fragment protection is necessary, such as in the study of penetrator interactions with reactive armor, or if a moderate penetrating x-ray capability is required. High-energy x rays are useful when the data desired are internal to the structure and significant penetrating x-ray capability is required. This division of the techniques according to energy is rather loose. Significant overlap does exist and, therefore, each new application deserves individual consideration.

LOW-ENERGY APPLICATIONS

The examples of low-energy x-ray applications given here used the Hewlett-Packard 150-keV flash x-ray system. The typical geometry used for multiple-exposure x rays is shown in Fig. 1. The heads are separated vertically to allow for image separation on the film. The object-to-source distance is usually 3 m and the object-to-film distance is usually 300 or 600 mm. Minimal protection is used on the heads and film so that the detail-revealing softest x rays are not absorbed.

* Pulsed High-Energy Radiographic Machine Emitting X Rays.

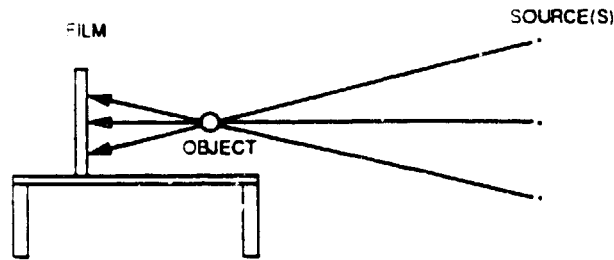


Fig. 1. Stacked x-ray heads for multiple exposures.

In the first example, the objective of the test was to image the low-density ejecta from the rear surface of a target as it was penetrated by a shaped-charge jet. The soft x-ray tubes have beryllium windows that do not absorb the lowest-energy x rays, and a window in the film cassette was covered with only Mylar and some low-density foam for shock absorption. Two layers of film-screen combinations were used in the cassette. The first film-screen layer absorbed nearly all the softest x rays. The soft x-ray radiograph, Fig. 2a, revealed a few larger particles and an encompassing cloud of very finely particulated material preceding the main portion of the jet. By comparison, the cloud of fine particles is not well resolved by the relatively hard x rays that exposed the second layer of film in the cassette, Fig. 2b. The soft x rays exposed details of the structure of the ejecta that we would otherwise have not been aware of.

The ring jet formation process is a double-collision process that produces very high velocity jet material. Figure 3 shows the ring-jet-producing device and an idealization of the collapse process. The driver system is detonated and drives the flyer plate into the shim in the entrance of the die. The shim is driven through the converging die and produces a ring jet near the wall of the die. At the centerline of the die, the ring jet then collapses on itself producing the secondary jet of interest. Radiography of the ring jet is demanding because of

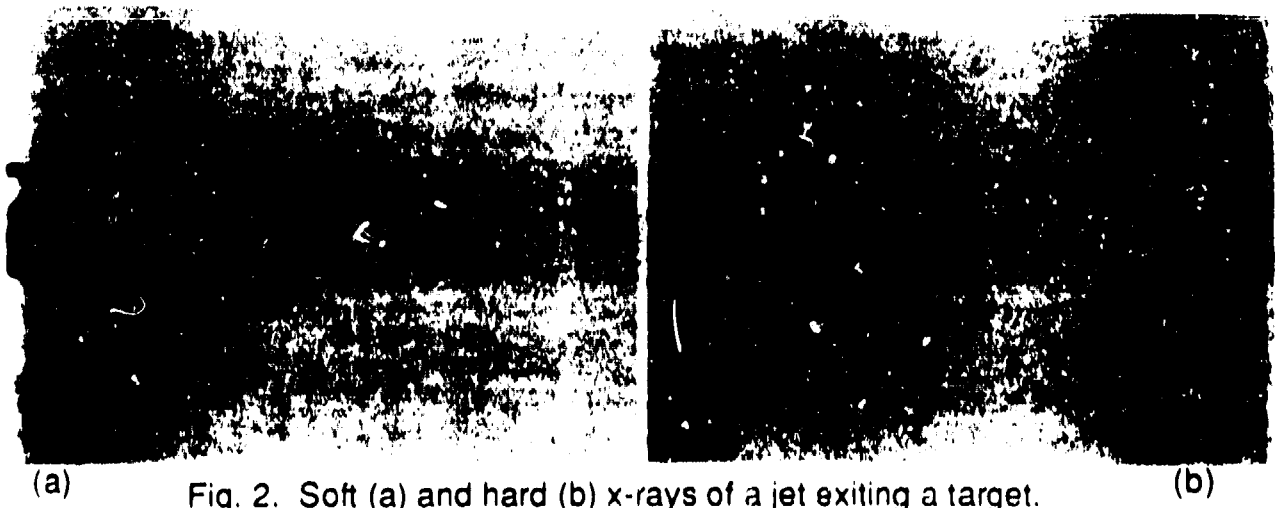


Fig. 2. Soft (a) and hard (b) x-rays of a jet exiting a target.

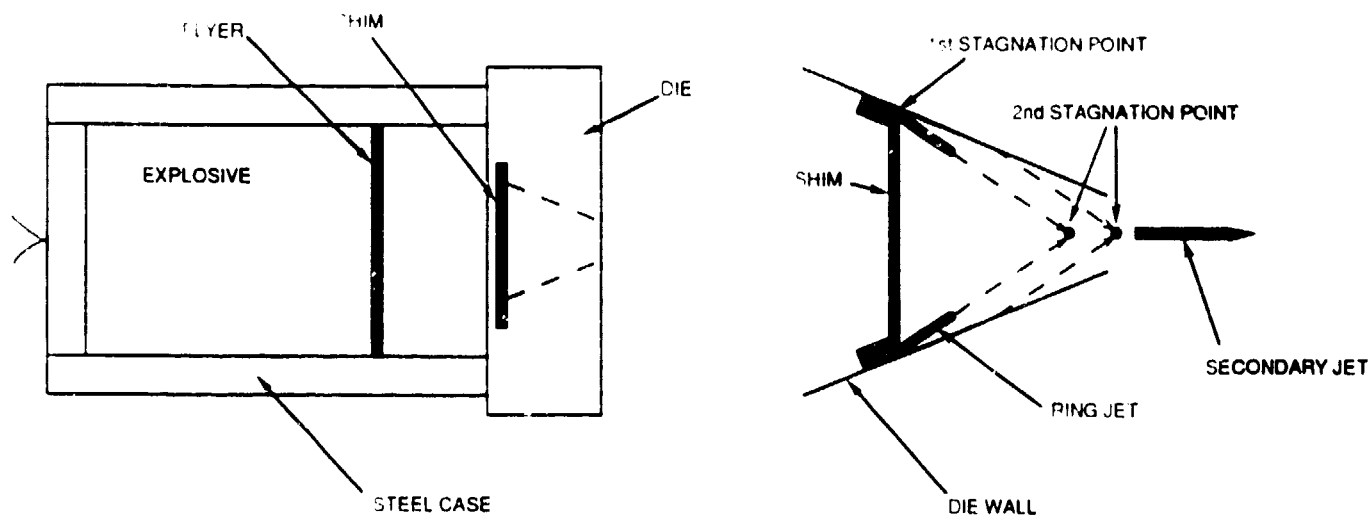


Fig. 3. Ring jet device (left) and idealized collapse process (right).

the high fragment field and large blast produced by the driver device, in conjunction with the small size and disperse condition of the jet.

Under certain conditions, the velocity of the second convergence of the ring jet is high enough that compressibility and/or thermal (phase-change) effects in the stagnation region cause the jet to become incoherent. Therefore, the radiographic objective was to observe the condition of the secondary jet. Because of the conditions created by the driver device, we decided to use a single pulse of the Hewlett-Packard 150-keV system and protect the equipment with large slabs of steel (3 ft by 3 ft by 3 in.) and numerous sandbags. Additionally, the front of the cassette had an aluminum cover. Figure 4 shows a radiograph of a tantalum ring jet (secondary jet) as it bifurcates. Although all the detail of the jet structure may not yet be resolved, the technique allowed us to determine the major characteristics of the relatively disperse jet, in spite of the high fragment field and blast produced by the driver device.



Fig. 4. Bifurcating ring jet.

MEDIUM-ENERGY APPLICATIONS

Medium-energy x rays are useful in obtaining shadowgraphs when significant cassette and x-ray head protection is required, and for penetrating radiography of relatively small or low-density objects. In the examples of medium-energy x-ray applications, we used geometric setups similar to that shown in Fig. 1 with 450-keV Hewlett-Packard systems or a single pulse from a 2.3-MeV Hewlett-Packard system. The object-to-source distance is usually 6 or 7 m and the object-to-film distance is usually between 600 mm and 1400 mm. The cassettes are protected by 1/2- to 3/4-in. (1.27- to 1.91-cm) aluminum covers for fragments and 1/2-in. (1.27-cm) Lexan for blast protection. The heads are protected by 1/2-in. Lexan.

A typical application is to determine the late-time characteristics of a jet or an explosively formed projectile (EFP). Figure 5 shows the radiograph obtained with the 450-keV system in a typical jet characterization experiment. The straightness, coherency, and other general characteristics of a jet can be directly observed. Measurements or estimates of the tip and tail velocities, the particulation time, the necking rate of instabilities, and the mass-velocity distribution can be made from radiographs such as these.



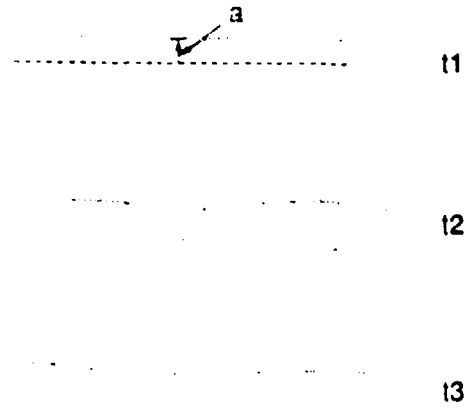
Fig. 5. Late-time radiograph of a particulating jet.

Figure 6a shows a segment of the jet shown in Fig. 5 as it particulates. The particle outline data obtained from digitizing the segments with a hand-held digitizing tablet are shown, along with the computed necking rate in Fig. 6b. This information can be related to the strength characteristics of the jet, through computer simulations of the particulation process.

The 450-keV units have enough penetration capability to resolve the condition of internal missile components contained by a thin skin (Fig. 7). This radiograph was used to evaluate the blast-shielding capability of the TOW flight motor for a tandem warhead system. Small warhead assemblies can be penetrated by the 450-keV machines as well. The collapse and subsequent jetting of a 12-mm-diameter shaped charge is shown in Fig. 8. In this case, the quality of the image was improved by collimating the x rays near the object to prevent multiple exposure of the film.



(a)



$$da/dt = -0.016 \text{ mm}/\mu\text{s}$$

(b)

Fig. 6. Radiograph of jet particulation (left) and digitized images and estimating necking rate (above right).



Fig. 7. Triple exposure of mock missile assembly.

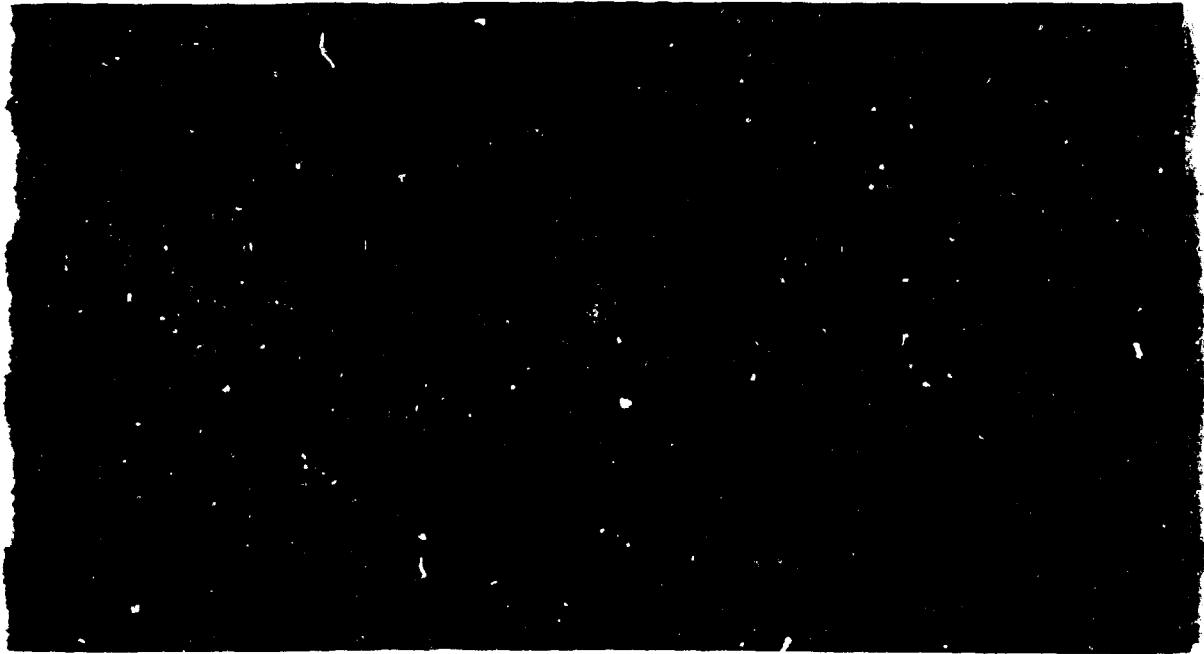


Fig. 8. Radiograph of the shaped-charge collapse process.

Another example of the usefulness of the penetration capability of medium-energy x rays is in the study of jet penetration of energetic materials such as propellant and explosives. The radiographs in Fig. 9 show the penetration of a fine-grained propellant by a jet. The location and shape of the reaction zone can be clearly seen, along with the jet.

When fragments or blast waves pose a hazard to x-ray film and heads, the cassette and head protection must be increased. When this is done, most of the penetration capability may be consumed by the protection, and the images obtained of most metals are shadowgraphs. However, the shadowgraphs obtained do provide valuable information. Figure 10 is a double exposure, taken with the Hewlett-Packard 2.3-MeV system, of a cased, hemispherical shaped charge before it was fired and shortly after firing. The static image provides a useful reference and the dynamic contains considerable detail, such as the condition of the jet and images of the fragments produced by the case.

The last example of medium-energy radiography applications is the estimation of a jet mass-velocity distribution from early-time shadowgraphs taken with the Hewlett-Packard 2.3-MeV system. The two radiographs shown in Fig. 11a were digitized with the hand-held digitizing tablet. The data were then integrated, assuming constant jet density, from the tip to the tail, to obtain the accumulated mass (Σm)-vs-position distribution. The mass point velocity (the velocity of a constant value of Σm) was then calculated using the known time difference between the exposures and the known position of the tip in each exposure. The mass-velocity distribution is labeled "SHADOWGRAPH" in Fig. 11b. This technique of estimating a mass-velocity distribution is due to Foster et al. at Eglin Air Force Base.

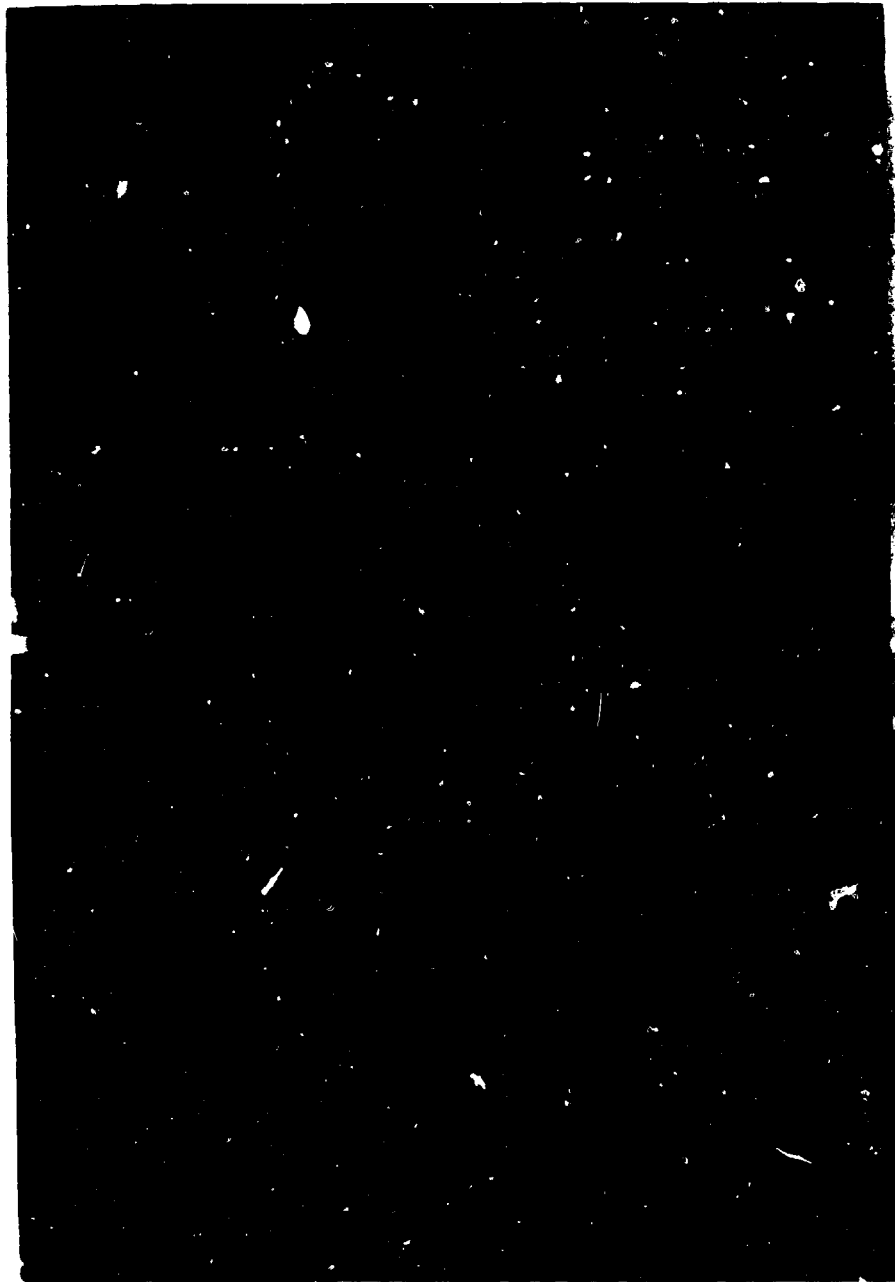


Fig. 9. Penetration of a fine-grained propellant by a jet.

HIGH-ENERGY APPLICATIONS

The examples of penetrating radiography given here were obtained at the PHERMEX and Ector facilities at Los Alamos. These machines produce significantly more radiation at significantly higher energy levels than the Hewlett-Packard machines applied in the previous examples. The Ector and PHERMEX machines produce a single pulse, and the source-to-object distance is usually about 1 m.

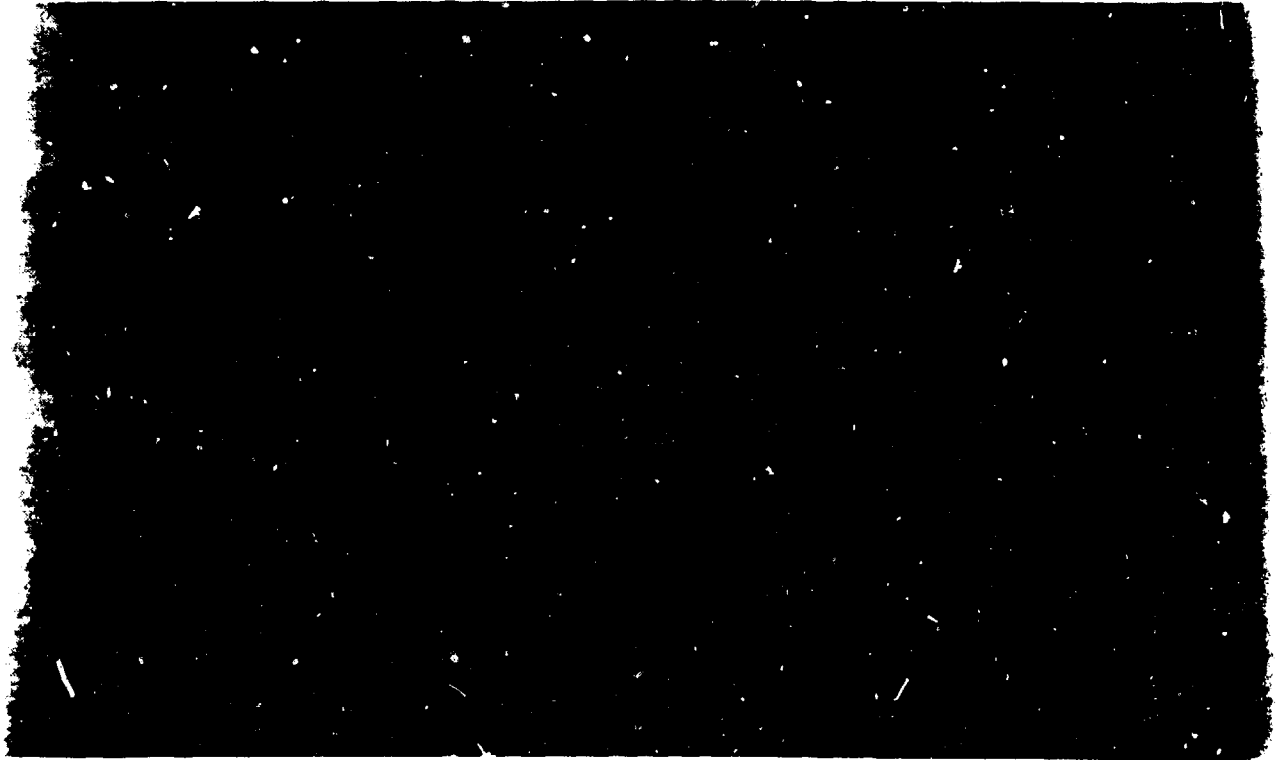


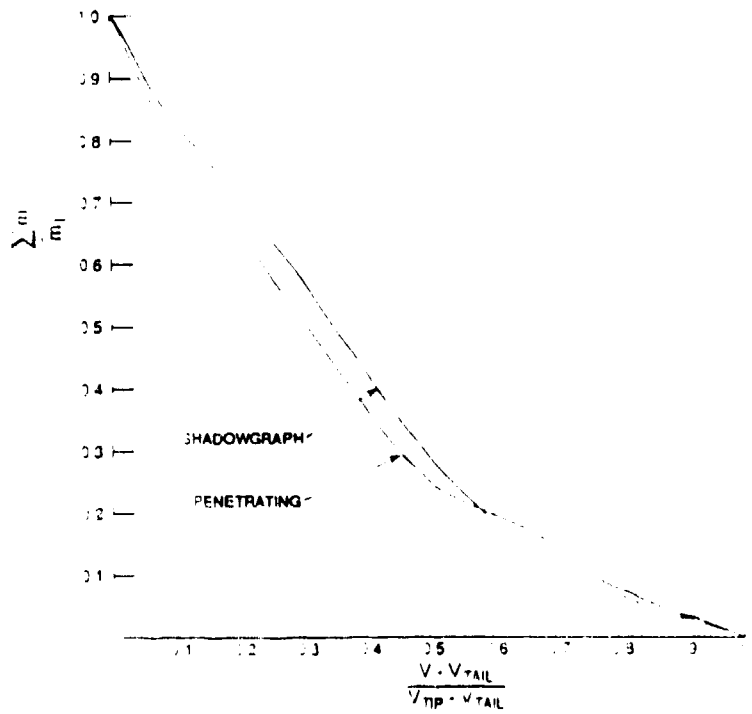
Fig. 10. Double exposure (static and dynamic) of a cased shaped charge.

The penetrating capability of these larger machines can be used to reveal some details of the internal structure of jets and EFPs. The jet shown in the upper image of Fig. 11a was radiographed by Ector at the same epoch of formation (Fig. 12a). This radiograph reveals a region of lower density in the center of the jet. The radiograph was digitized by a scanning microdensitometer and the numerical data analyzed to give the tomographic reconstruction in Fig. 12b. The reconstruction shows that the material in the low-density region is rarefied to about half the nominal density of the metal. A later-time Ector radiograph of the same jet indicates that the low-density region "heals" itself. The density profiles obtained with the analysis of the Ector radiographs were approximated by mathematical functions and used in the integration routines to obtain the curve labeled "PENETRATING" in Fig. 11b. The comparison shows that although the penetrating x ray revealed the low-density region, the mass-velocity distribution estimated from the shadowgraph was not drastically in error.

The aerodynamic stability of an EFP is determined by the position of the center of pressure, relative to the center of mass. The center of pressure can be estimated, when the velocity and outer shape of the EFP are known, but the internal contour must be known to accurately estimate the center of mass. An Ector radiograph of a Honeywell EFP, Fig. 13, clearly defines the inner contour. The tomographic reconstruction of this radiograph allowed an accurate estimate to be made of the center of mass of the EFP.



(a)

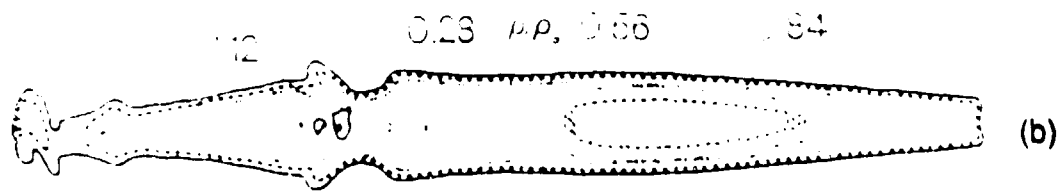


(b)

Fig. 11. Early-time radiographs (a) of a jet; mass-velocity distribution (b) calculated from radiographic data in (a).



(a)



(b)

Fig. 12. Penetrating radiography (a) of a jet; tomographic reconstruction (b).



Fig. 13. Penetrating radiography of the Honeywell EFP.

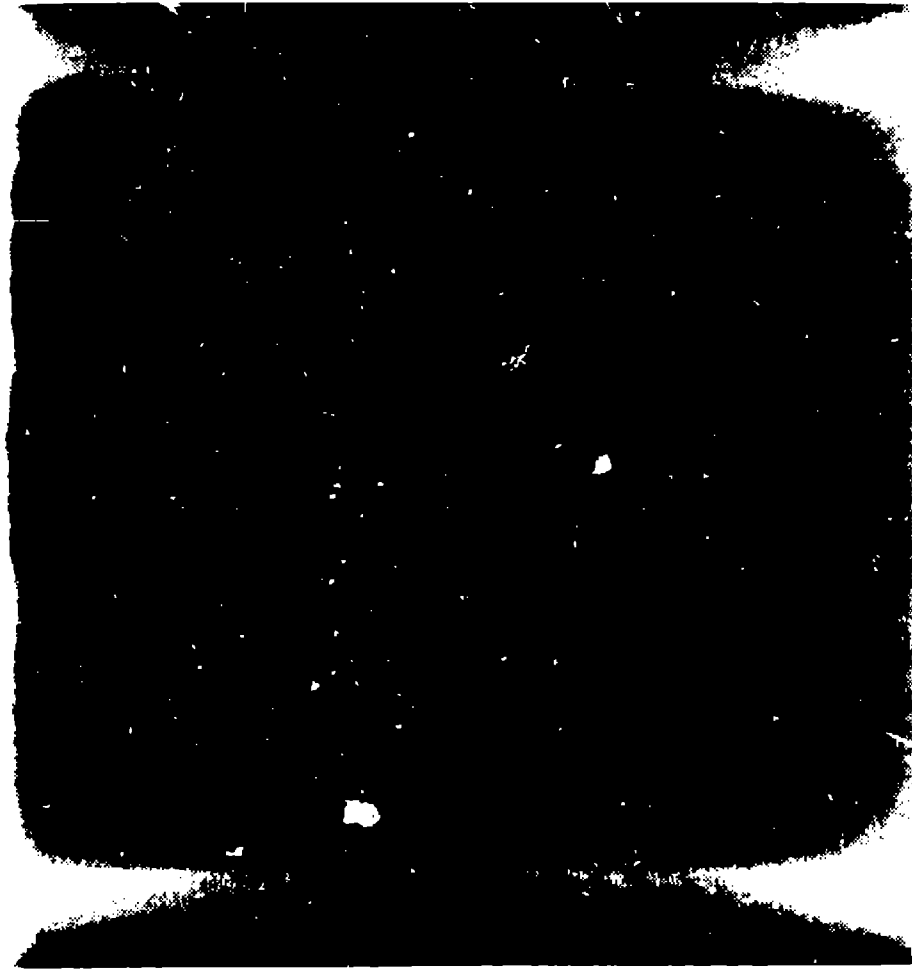


Fig. 14. Penetrating radiography of a jet penetrating a target.

The mechanics of target penetration by jets, EFPs, and rods can be examined by penetrating radiography. Figure 14 is a radiograph obtained with the PHERMEX machine that shows the penetration of a target made from a filled cylindrical tube of areal density 410 g/cm^2 . This is equivalent to observing a jet behind a 2-in. (5-cm) steel plate. Thus, many details are revealed by penetrating radiography even in situations involving small variations in object density.

ACKNOWLEDGMENTS

The Los Alamos researchers who have been involved with the radiography discussed in this paper are listed here: M. L. Price (Figs. 5, 6, and 11); D. B. Fradkin (Fig. 7); G. W. Laabs (Fig. 8); B. W. Asay (Fig. 9); M. J. Gumbert (Fig. 10); R. R. Karpp (Figs. 12-14); and L. A. Schwalbe (Fig. 13). The author gratefully acknowledges their cooperation and assistance.

LAWRENCE M. HULL

Explosives Applications Group, M-8
Dynamic Testing Division
Los Alamos National Laboratory

Dr. Hull received a B.S. in Mechanical Engineering from Colorado State University in 1977, an M.S. in Mechanical Engineering from the Massachusetts Institute of Technology in 1980, and a Ph.D. in Mechanical Engineering from the Massachusetts Institute of Technology in 1982.

He is currently involved in the study of the hydrodynamics of penetrators for conventional warheads. He conducts experiments to evaluate shaped-charge jet performance against modern armor technology and to develop and support models of jet formation and jet-target interactions.

